ICSV14
Cairns • Australia
9-12 July, 2007
14th International Congress on Sound & Vibration

IMPACT PROPERTY AND POST IMPACT VIBRATION BETWEEN TWO IDENTICAL SPHERES

Hirofumi MINAMOTO[1], Keisuke SAITOH and Shozo KAWAMURA

[1]Toyohashi University of Technology Dept. of Mechanical Engineering
Hibarigaoka 1-1. Tempaku-cho, Toyohashi, 441-8580 Japan
minamoto@mech.tut.ac.jp (email address of lead author or presenter)

Abstract

Contact and impact of spheres are fundamental and important problem in engineering. The severity of impact is generally characterized by the Coefficient of Restitution. However, deformed bodies after impact keep vibrating elastically. This paper deals with the direct central impact of two identical spheres and investigates the impact properties and post impact vibration. For this purpose, experiments and numerical simulations were carried out. The experimental and analytical results were compared and they matched quite well about their macro-mechanical quantities such as coefficient of restitution and contact time. On the post impact vibration, the effective value of the sphere center velocity increases with impact velocity but the frequency does not depend very much on the impact velocity.

1. INTRODUCTION

When an impulsive force act on a body, the body changes its rigid body motion depending on the impulse. Bodies repel after impact due to the elasticity in general. This kind of change in rigid body motion can be evaluated by the macro-mechanical impact properties such as coefficient of restitution and contact duration. Therefore, in multibody dynamics, it is essential to understand the impact properties for the bodies.

Generally, the deformations due to impulsive forces propagate inside the body with time. The place where the strain exceeds the elastic limit, inelastic deformation occurs and the corresponding energy is dissipated. The rest of elastic strain is transformed into kinetic energy and elastic vibration. The vibration of the body after impact deteriorates the quality of the motion control and positioning accuracy and cause a noise.

From these points of view, impact properties and post impact vibration of the bodies are one of the important subjects in mechanical dynamics. There are many researches reported so far [1]-[7] . Especially, spheres are treated experimentally and theoretically very much, since they are one of the fundamental mechanical element. However, the experimental works which have done before are limited to the low speed impact and less information is available on the used materials.

The authors have already dealt with the impact between two identical steel spheres made of JIS SUJ2 steel (Japan Industrial Standard, Steel for Use in Journal bearing). Then, the finite element simulations were carried out [7]. This paper deals with the sphere of typical light metal, aluminium (JIS A5052), and compare the impact properties with those of SUJ2 steel. Then the finite element simulations are carried out and the results are compared with those of the experiments. Then the post vibration of the sphere center is investigated.

2. IMPACT EXPERIMENTS BETWEEN TWO IDENTICAL SPHERES

The spheres of 1in (25.4mm) diameter were used for the experiments for both SUJ2 steel and A5052 aluminium materials. Since the spheres experienced surface hardening during production process, the spheres were annealed under 850 degree-Celsius for SUJ2 and 350 degree-Celsius before experiments.

Two experimental setups were used for the experiments depending on the impact speed. For low speed impact V_i=~3m/s, the spheres were impacted by pendulum set up as shown in Fig.1. The angles of pendulums before and after impact were measured and the coefficient of restitution was calculated from the next equation.

$$e = \frac{\sqrt{1-\cos\theta_2} - \sqrt{1-\cos\theta_1}}{\sqrt{1-\cos\theta_0}} \tag{1}$$

where, θ_0, θ_1 indicate the angle of impacting pendulum before and after impact, respectively and θ_2 indicates the angle of impacted pendulum after impact. Also, contact duration was measured from the conducting line attached on the each sphere.

For high speed impact V_i=10m/s~, the spheres were impacted by air gun set up as shown in Fig.2. Two spheres were placed in line at rest in an acryl pipe of inner diameter 26mm and length of 400mm. The one of two spheres was ejected by air pressure against the other sphere. The appropriate holes were placed on the pipe to bleed and relief the air pressure.

Pairs of laser beam pointer and photo transistors were set along the pipe as shown in Fig.2(a). When the spheres pass through the photo transistors, the output voltages of the photo transistors show the pulses. The initial speed of impacting sphere V_{10} and post impact speed of the both spheres V_1 and V_2 were obtained from the time of the pulses and the distance between the photo transistors. The coefficient of restitution between two spheres was given by next expression.

$$e = \frac{V_2 - V_1}{V_{10}} \tag{2}$$

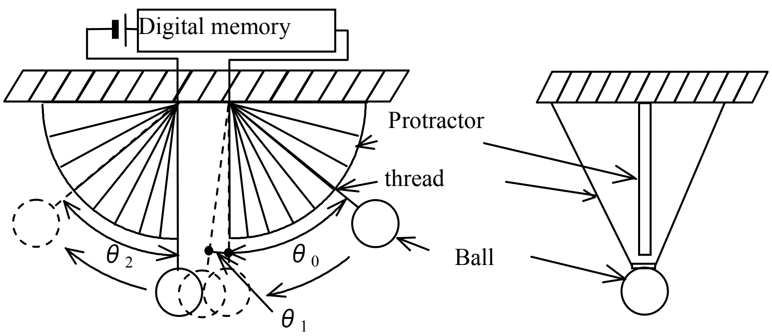

Figure 1.Low speed impact setup

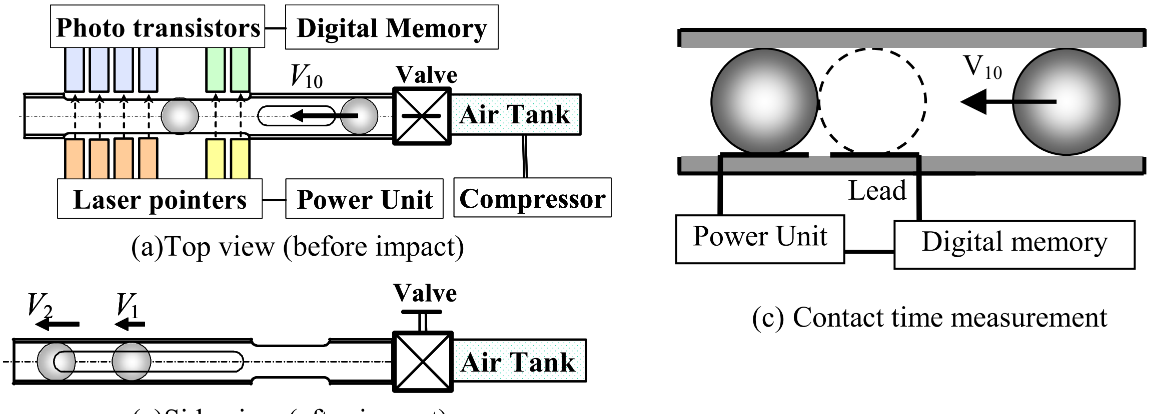

(a)Top view (before impact)

(a)Side view (after impact)

(c) Contact time measurement

Figure 2.High speed impact setup

Contact duration of the spheres were obtained by the closing time of the circuit composed of two fine conductive line set on the bottom surface of the pipe as shown in Fig.2(c). The one of two conducting line was set just under the stationary sphere and the other line was set just before the stationary sphere. The lines are connected to the electrical power source and the circuit opens before impact. When the ejected sphere contacts with the stationary sphere, the circuit closes.

The deformation (compression) Δd and contact circle diameter a were measured after impact. The definition of the deformation and contact circle diameter are shown in Fig.3.

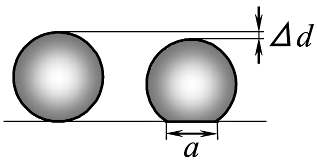

Figure 3.Contact circle diameter and sphere deformation

3. MATERIAL PROPERTIES

To identify the material properties of SUJ2 steel and A5052 aluminium, static material test and split Hopkinson Pressure Bar (SHPB) test were conducted. Before the experiments, annealing was made to the test pieces under the same condition to the spheres. The stress-strain curves are shown in Fig.4 (a) and (b) for SUJ2 steel and A5052 aluminium, respectively. It is clearly observed that the stress levels of the stress-strain curves increase with the strain rate. This is the strain rate dependency of these materials.

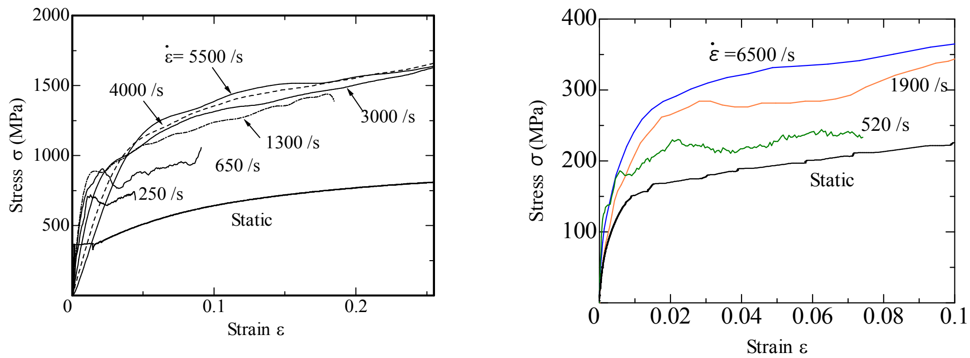

(a)SUJ2 material

(b)A5052 material

Figure 4. Stress-Strain curves

4. SIMULATIONS OF IMPACT BETWEEN TWO IDENTICAL SPHERES

The impact of sphere of 1in (25.4mm) diameter was simulated numerically by Finite Element Analysis (F.E.A.). General non-linear dynamic F.E.A. software LS-DYNA [8], [9] was used for the impact simulations. In case of one dimensional impact between two identical spheres, the force transmission and deformation are symmetrical on the contact surface according to the Newton's third law. Therefore, the one-dimensional impact of two identical spheres can be replaced equivalently by the impact of a ball against a rigid plane. Here, the relative impact speed between two identical balls V_i should be twice of the ball speed against rigid plane $2V_0$.

It was observed from the experimental measurements that the shape of contact plane after impact was almost circle. Therefore, the variation of radial deformation along circumferential direction is negligible. The impact of a sphere to rigid plane can be treated by axi-symmetric analysis. Four-node axi-symmetric elements are used for the finite element model shown in Fig.5. Figure 5(a) shows the whole finite element mesh used for SUJ2 sphere. The total number of nodes and elements are 3837 and 3742, respectively. The area around contact region was meshed finely as shown in Fig.5 (b). The size of the smallest element is about 0.6mm. The finely meshed area was extended for the mesh of A5052 sphere since the larger contact region will be expected. The total number of nodes and elements are 9280 and 9414, respectively for A5052 sphere.

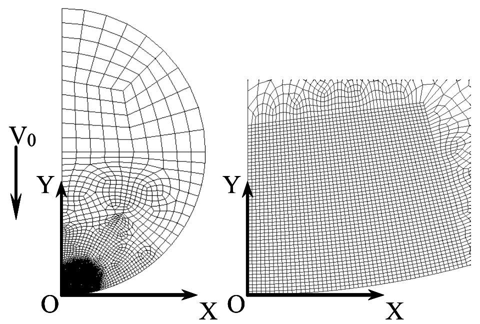

(a) Entire subdivision (b)Fine meshed area
Figure 5. Finite Element subdivision

Table 1. Material properties

	SUJ2	A5052
Density (kg/m^3)	7825	2640
Young's modulus (GPa)	206	77
Poisson's ratio	0.3	0.33
Initial yield stress (MPa)	350	101

Piecewise Linear Isotropic Plasticity model (Model 24) was used for the material model [8]. This model is one of the most general material models prepared in LS-DYNA and it can consider the strain rate sensitivity of material properties. The constitutive law used in this model is the following relation [9].

$$s_{ij}^{\nabla} = 2G\dot{\varepsilon}'_{ij} \qquad (i, j = x, y, z) \tag{3}$$

where, s_{ij}^{∇} ,G, $\dot{\varepsilon}'_{ij}$ indicate Jaumann rate of deviatoric stress, transverse elastic modulus and deviatoric strain, respectively. von Mises criterion was used for yielding and the yielding function is expressed in the next equation.

$$\phi = \frac{1}{2} s_{ij} s_{ij} - \frac{1}{3}\sigma_y^2 \tag{4}$$

The summation convention for tensor operation was applied on the subscript *i* and *j* in the above equation. σ_y indicates dynamic yield stress and it is given by the next form.

$$\sigma_y = \beta\left(\dot{\bar{\varepsilon}}^p\right)\sigma_{y\,staic} \tag{5}$$

where, $\beta\left(\dot{\bar{\varepsilon}}^p\right)$ is called scale factor. It is a function of effective plastic strain rate $\dot{\bar{\varepsilon}}^p$ and expresses the increase of dynamic yield stress with strain rate. Figure 6 shows the scale factor derived from the stress-strain curves in Fig.4.

The stress-strain relation after yielding was derived from the static tensile stress-strain curve by approximating the curve by piecewise lines. The stress level of this curve is shifted depending on the strain rate in accordance with the scale factor β shown in Fig.6.

Contact force is calculated by Penalty method. Under the above conditions, numerical simulations were carried out. Coefficients of restitutions were calculated from the next relation.

$$e = -\frac{V_1}{V_0} \tag{6}$$

where, V_0 and V_1 indicate the speeds of initial impact and after impact of sphere center.

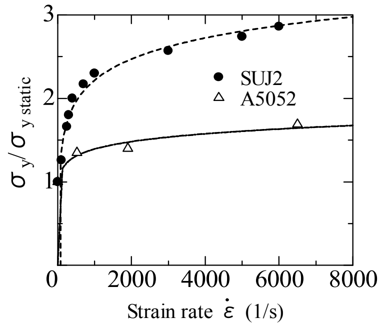

Figure 6.Scale factor

5. RESULTS AND DISCUSSIONS

5.1 Impact properties

Figure 7 shows the relation between the coefficient of restitution and relative impact velocity. Figure 8 shows the relation between the contact duration and relative impact velocity. It is seen from these figures that the experimental and the simulation results match well. The coefficients of restitution decrease rapidly in low speed range and also decrease slowly in high speed region for the both materials. Further, it is found that SUJ2 sphere has higher coefficient of restitution than A5052 sphere. The contact duration also decrease rapidly in low speed range. The difference of contact duration between SUJ2 sphere and A5052 sphere is small.

Figure 9 shows the relation between relative impact velocity and compressive deformation of the spheres Δd . Figure 10 show the relation between relative impact speed and contact circle diameter *a*. It is seen from these figures that the experimental results and the simulation results shows a good corresponding. The deformation of the sphere increases linearly with the relative impact velocity. The contact circle diameter increase rapidly in low speed region and after that it increase slowly with relative impact speed. For both the deformation and the contact circle diameter, A5052 sphere has larger values than those of SUJ2 sphere.

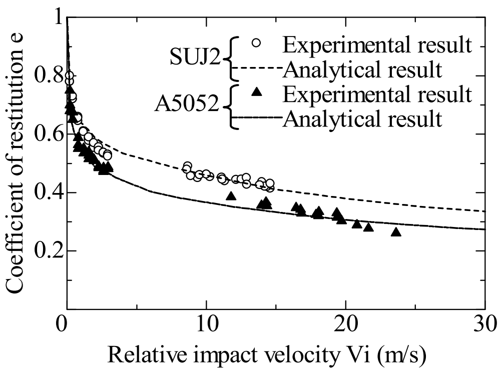

Figure 7. Coefficient of restitution

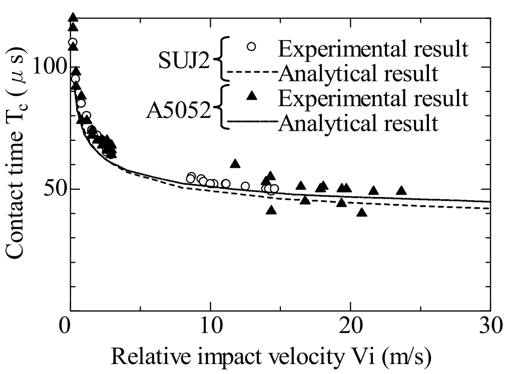

Figure 8. Contact duration

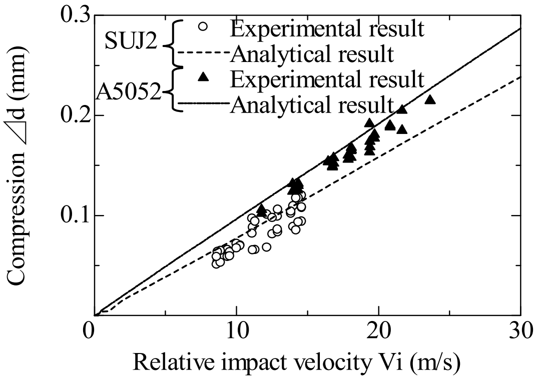

Figure 9. Compression of sphere

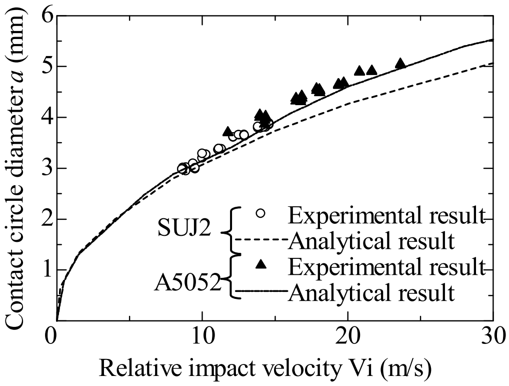

Figure 10. Contact circle diameter of sphere

Then the sphere behaviour during impact is considered. The case of relative impact speed V_i=10m/s is picked up as a representative case.

Figure 11 shows the contact force- deformation diagram. The diagram draws a hysteresis due to the inelastic deformation. SUJ2 sphere has larger contact force and smaller deformation than those of A5052 sphere. This is because of their 0.2% proof stress (yielding stress) and yielding strain. And the difference of slope of the diagram in repulsive phase is come from the difference of their Young's modulus.

As shown in Fig.12, the contact forces increase with time in compression phase and reaches to the maximum force at 29 μs for SUJ2 sphere and 36 μs for A5052 sphere. Then the contact force decrease with time in repulsive phase. In case of perfectly plastic body, the maximum deformation and the maximum contact force occurs at the same time. But as shown in Fig.12, the compression phase is longer than the repulsive phase due to inelastic deformation.

As shown in Fig.13, the displacements of the sphere center reach to the maximum deformation at 33 μs for SUJ2 sphere and 40 μs for A5052 sphere. After the maximum deformation, part of the deformation is recovered elastically in repulsive phase.

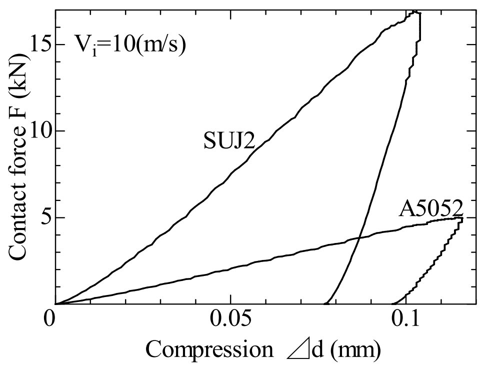

Figure 11.Force-deformation diagram

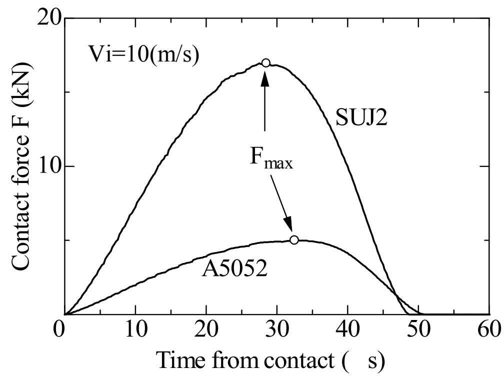

Figure 12.Variation of contact force with time

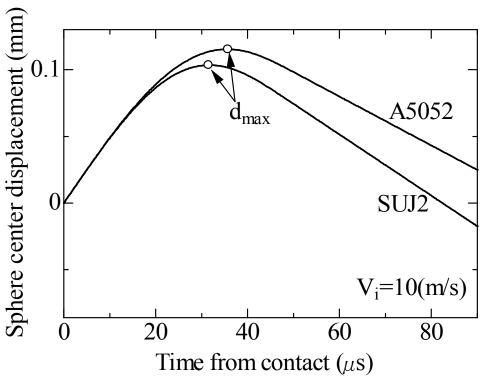

Figure 13.Variation of deformation with

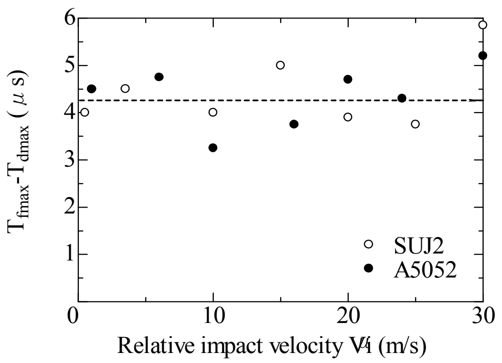

Figure 14.Time difference

From the above consideration, it is seen that the maximum contact force and maximum deformation of the SUJ2 sphere occur at 29 μs and 33 μs, respectively. Also, those for the A5052 sphere occur at 36 μs and 40 μ s, respectively. It shows that there exists the time difference between the deformation and the contact force. Since the stiffness varies with the deformation speed due to the strain rate sensitivity, it causes the effects like a kind of viscous damping. This is so-called material damping.

Figure 14 shows the relation between the relative impact velocity and the difference of the time of maximum contact force T_{fmax} and maximum deformation T_{dmax}. It is seen that the value of time difference is around 4 μs regardless of the relative impact speed.

5.2 Post impact vibration of sphere center

As mentioned in Chap.1, post impact vibration has an influence to the post impact motion of the sphere. Therefore, the vibration of the velocity of sphere center is investigated in this paper.

Figure 15 shows the variation of the velocity of the sphere center with time for V_i=10m/s. It is clear that the velocity of the sphere center vibrate after impact.

Figure 16 shows the relation of the effective value of the sphere velocity and the impulse. It is seen that the effective value increases with impulse. The values of the inelastic impact are larger than that of elastic impact.

Figure 17 shows the post impact frequencies of the sphere center velocity for SUJ2 sphere and A5052 sphere. The frequencies are similar for SUJ2 sphere and A5052 sphere regardless of the relative impact velocity. It is thought that the vibrations of the spheres are in the natural vibration and the frequency is around the natural frequency of the spheres. However, the detail analyses by FFT have to be done in the next step.

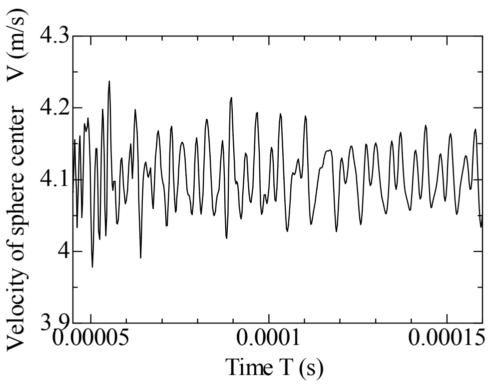

Figure 15.Variation of velocity of sphere center after impact

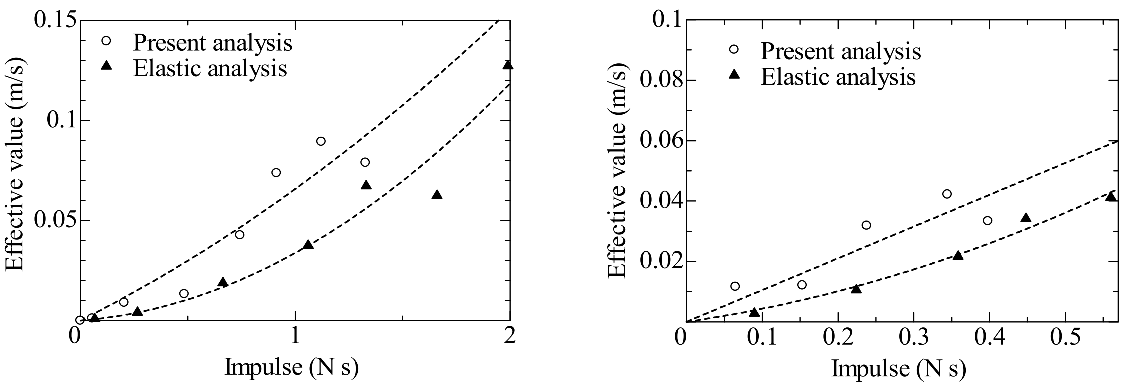

(a)SUJ2 (b)A5052

Figure 16.Variation of effective value with impulse

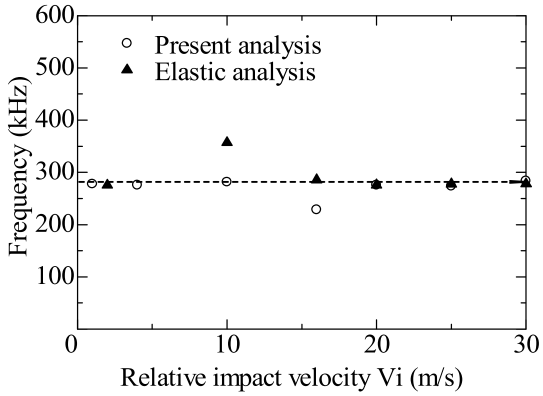

(a)SUJ2

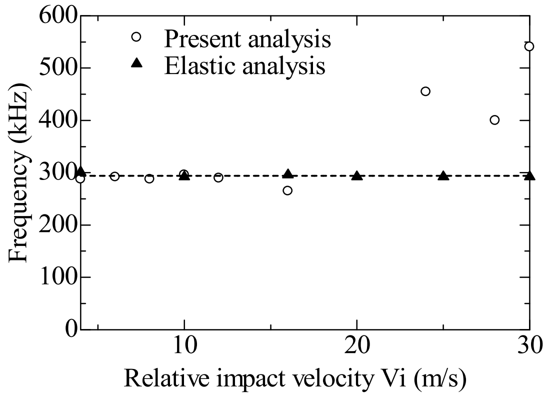

(b)A5052

Figure 17.Post impact frequency of sphere center velocity

6. CONCLUSIONS

In the present paper, impact experiments of two identical spheres were conducted and impact properties of the spheres was examined. Impact analyses by considering the strain rate effect were conducted by finite element method. The experimental results and analytical results were compared, and then the post impact vibration of the sphere center was considered. The followings were understood as a result.

(1) The results of the analyses by finite element method and the impact experiments matched well.

(2) In strain rate dependent material, phase shift caused between deformation and contact force by the influence of material damping.

(3) On the post impact vibration, the effective value of the sphere center velocity increase with impulse which acts during impact.

REFERENCES

[1]Tatara, Y., Moriwaki, N., Study on Impact of Equivalent Two Bodies : Coefficients of Restitution of Spheres of Brass, Lead, Glass, Porcelain and Agate, and the Material Properties, *Bulletin of Japan Society of Mechanical Engineers*, Vol.**25**,No.202(1982),pp.631-637.

[2] Villaggio, P., The Rebound of an Elastic Sphere Against a Rigid Wall, *Transactions of the ASME,Journal of Applied Mechanics*, Vol. **63** (1996),pp. 259-263.

[3]Thornton,C.,Coefficient of restitution for collinear collisions of elastic-perfectly plastic spheres, *Transactions of the ASME*, *Journal of Applied Mechanics*, Vol.**64** (1997), pp.383-386.

[4] Seifried, R., et al., Numerical and experimental evaluation of the coefficient of restitution for repeated impacts, *International Journal of Impact Engineering*,Vol.**32** (2005), pp.508-524

[5] L. Vu-Quoc,X. Zhang,L. Lesburg, A Normal Force-Displacement Model for Contacting Spheres Accounting for Plastic Deformation: Force-Driven Formulation, *Transactions of the ASME,Journal of Applied Mechanics*, Vol. **67** (2000),pp. 363-371.

[6]Chuan-Yu Wu, et al., Energy dissipation during normal impact of elastic and elastic-plastic spheres, *International Journal of Impact Engineering*, Vol.**32**(2005), pp.593-604.

[7]Minamoto, H., Elasto / Visco-plastic impact of two equivalent spheres made of SUJ2, *Transactions of the Japan Society of Mechanical Engineers, Series C*, Vol.**71**,No.701 （2005）, pp.51-57（in Japanese）.

[8] *LS-DYNA KEYWORD USER'S MANUAL*, Version 950, Livermore Software Technology Corporation, (1999).

[9] *LS-DYNA THEORETICAL MANUAL*, Livermore Software Technology Corporation, (1998).